International Journal of Heat and Mass Transfer 53 (2010) 3629–3637

Contents lists available at ScienceDirect

International Journal of Heat and Mass Transfer

journal homepage: www.elsevier.com/locate/ijhmt

A multi-layer porous wall model for coronary drug-eluting stents

Giuseppe Pontrelli [a,*], Filippo de Monte [b]

[a] Istituto per le Applicazioni del Calcolo – CNR, Via dei Taurini 19, 00185 Roma, Italy
[b] Dipartimento di Ingegneria Meccanica, Energetica e Gestionale University of L'Aquila, Località Monteluco, 67040 Roio Poggio (AQ), Italy

ARTICLE INFO

Article history:
Available online 12 May 2010

Keywords:
Mass transfer
Multi-layered porous media
Advection–diffusion equation
Multi-layer penetration depth
Drug delivery
Pharmacokinetics

ABSTRACT

An analytical solution for solving the transient drug diffusion in adjoining porous wall layers faced with a drug-eluting stent is presented. The endothelium, intima, internal elastic lamina and media are all treated as homogeneous porous media and the drug transfer through them is modelled by a set of coupled partial differential equations. The classical separation of variables method for a multi-layer configuration is used. The model addresses the concept of penetration depth for multi-layer solids that is useful to treat the wall thickness by estimating a physical bound for mass diffusion. Drug concentration level and mass profiles in each layer at various times are given and discussed.

1. Introduction

Alteration of blood flow due to the narrowing or occlusion of an artery is one of the most common occurrences in cardiovascular diseases. A medical treatment involves the insertion of a wire scaffold, or stent, designed to hold open and to provide structural stability to the injured vessel. Often such a treatment reveals ineffective and failure is associated with the growth of tissue through the wires of the stent, that reoccludes the lumen [1]. This can be prevented by a local and controlled delivery of drugs which inhibit tissue growth. Such a drug is contained in a thin porous polymeric layer coating the stent surface (drug-eluting stent, DES for short) and is aimed at healing the vascular tissues or at preventing a possible restenosis by virtue of its anti-proliferative action against smooth muscle cells.

The design of DES is aimed at a prolonged release of the drug, and mathematical models are proposed to simulate the mass transport in the arterial wall and the complex mechanism of drug elution. The drug is transported through the vessel wall by both convective and diffusive processes, and might be metabolized in the tissues and its progress arrested by partitioning. Computational modelling is an important tool for deeper understanding the physical factors that influence the transport process, namely the geometrical design of the stent, the mechanical characteristics of the materials, and the chemical properties of the drug [2]. These effects combine in different time–space scales and physics and need integrative biomechanical methods [3]. In the last years, a number of mathematical models have been developed to address the fundamental problem of the mass release from DES through the arterial wall [4–6]. Unconventional approaches of drug delivery, such as those based on the endoluminal gel paving technology, have been recently proposed [7]. In some work the combination of solid mechanics and fluid dynamics allows both mechanical expansion and DES elution properties to be investigated [8]. Difficulties in coupling different geometrical scales have been reported [9], and have been recently overcome by multiscale strategies [10]. In most of these studies, the complex multi-layered structure of the wall is disregarded and a homogeneous porous material with averaged properties (i.e. media) has been considered for simplicity.

On the other hand, it is known that the arterial wall is constituted of many layers with different structural and chemical properties [11,12] and it is believed that a more effective description of mass release is obtained with a more accurate modelling of the wall structure. According to the classification of Prosi et al. there are usually three categories of models depending on the level of description of arterial wall [9]. The *wall-free model* describes the arterial wall simply by means of suitable boundary conditions. The *fluid-wall model* approximates the wall structure by a single homogeneous layer. Though better than the wall-free model, it is still inaccurate, as misses important details of tissue microstructure that can play into drug release mechanism. The *multi-layered model* is the most complete model which takes into account the heterogeneous properties of the different layers constituting the wall but, due to its complexity, a larger number of parameters is required to characterize the physical properties of each layer. Such a comprehensive model would depend on so many variables that, if not conveniently simplified, it raises more questions than useful answers. An appropriate degree of simplification is necessary to

* Corresponding author.
E-mail addresses: pontrelli@iac.rm.cnr.it (G. Pontrelli), filippo.demonte@univaq.it (F. de Monte).

0017-9310/$ - see front matter © 2010 Elsevier Ltd. All rights reserved.
doi:10.1016/j.ijheatmasstransfer.2010.03.031

Nomenclature

c	mass volume-averaged concentration
D	drug diffusive coefficient
J	mass flux
k	partition coefficient
l	layer thickness
d^*	penetration distance or penetration depth
t^*	penetration time
m	boundary accuracy index (BAI)
M	dimensionless mass per unit of area
P	membrane permeability coefficient
t	time
x	space coordinate
X_i	eigenfunction

Greek symbols

γ	diffusivity ratio: $\frac{D}{D_{max}}$
ϵ	medium porosity
λ	eigenvalue
σ	material ratio: $\frac{k\epsilon}{(k\epsilon)_{max}}$
ϕ	nondimensional permeability: $\frac{Pd^*}{D_{max}(k\epsilon)_{max}}$
θ	fraction of drug mass: $\frac{M}{M_0(0)}$

Subscripts

0	0-th layer (coating)
i	i-th wall layer
n	number of layers

discern the relevant features of the phenomena. Although the complexity of stent geometry would require the use of 3D models [5], nevertheless in fundamental studies simpler one-dimensional models give some useful hints on the basic physics and allow a systematic analysis on a wide range of parameters. The easier handling of the governing equations leads to an explicit analytical form of the solution and gives a deeper insight into the transport process. In a recent paper, a mathematical model for the mass diffusion from the coating into the arterial tissue as a fluid-wall model has been presented and the strong analogy with heat diffusion processes has been emphasized [4]. The influence of other effects such as the plasma filtration velocity and the drug absorption have been investigated in [13].

In the present work, a multi-layered extension of the above studies is developed. Following [11,14], an idealized model of wall consisting of four layers (namely endothelium, intima, internal elastic lamina and media) is proposed. Each layer is treated as a macroscopically homogeneous porous medium with own diffusive properties and continuity of mass flux between any two adjacent layers is imposed (the geometrical and mechanical effects of the stent are not considered here). As a matter of fact, the endothelium is covered by a thin ciliate layer called endothelial surface layer or glycocalyx, constituted by a sequence of long chain macromolecules and proteins [12]. As the drug transport properties through the glycocalyx are unknown, it has been included in the endothelium layer for simplicity. The stent coating is assumed as a thin porous slab in imperfect contact with the endothelium due to the presence of a topcoat. The adventitia and the surrounding tissues form the outmost wall layer and have a sufficiently large thickness to be considered as semi-infinite (Section 2). However, by using the concept of penetration depth defined in transient heat conduction [15] and extending it to the present multi-layered problem, we estimate the correct distance where the concentration and mass flux are dumped out and approximate this semi-infinite layer as a bounded region (Section 3). The classical separation of variables method leads to a Sturm–Liouville problem with discontinuous coefficients and severe spectral irregularities (Section 4). Drug concentration in each layer at various times is given in the form of a Fourier series by using dimensionless parameters which control the transfer mechanism across the layered wall (Section 5). The concentration levels and the mass profiles are shown and discussed in Section 6. In particular, the drug diffusivity in the wall layers is shown to greatly influence the residence time.

The aim of these studies is to enhance control of the rate of drug delivery, enable a wider range of drug therapies, and increase the range of clinical applications of DES.

2. The multi-layer wall model: governing equations

A drug-eluting stent (DES) consists of a tubular wire mesh (*strut*), inserted in a stenosed artery and coated with a thin layer (*coating*) of biocompatible polymeric gel containing a therapeutic drug to be delivered (Fig. 1).

Let us consider a stent coated by a thin layer (of thickness l_0) of gel containing a drug and embedded into the arterial wall [6]. Because most of the mass dynamics occurs along the direction normal to the stent coating (radial direction), we restrict our study to a simplified 1D model. In particular, we consider a radial line crossing the metallic strut, the coating and the arterial wall and pointing outwards and, being the wall thickness very small with respect to the arterial radius, a cartesian coordinate system x is used along it. It is generally accepted that the arterial wall is constituted by a sequence of contiguous layers of different physical properties and thickness, say the endothelium, the intima, the internal elastica lamina (IEL), the media and the adventitia (see [16] for an anatomic and physiological description of them). Either the polymer coating and the wall layers are treated as macroscopically homogeneous porous media. Without loss of generality, let us assume $x_0 = 0$ is the coating-wall interface. In a general 1D framework, let us consider a set of intervals $[x_{i-1}, x_i]$ $i = 0, 1, 2, \ldots, n$ having thickness $l_i = x_i - x_{i-1}$ modelling the coating (layer 0) and the wall (layers 1,2,...,n) (Fig. 2).

At the initial time ($t = 0$), the drug is contained only in the coating and it is distributed with maximum, possibly nonuniform, concentration $C_0 f_0(x)$ and, subsequently, released into the wall. Here, and throughout this paper, a mass volume-averaged concentration

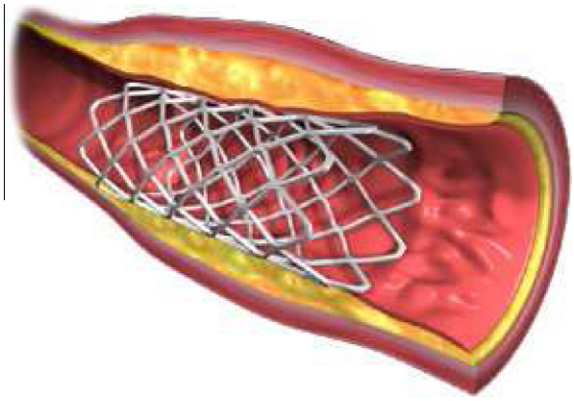

Fig. 1. A drug-eluting stent implanted in a stenotic artery.

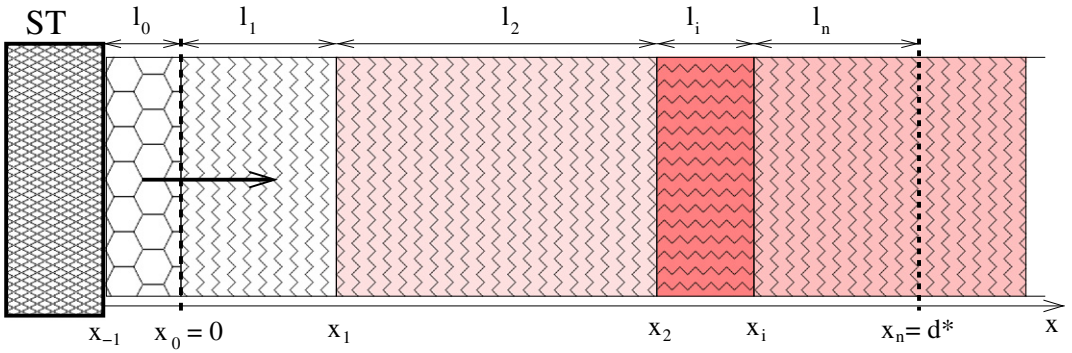

Fig. 2. A sketch of the layered wall. The 1D wall model is defined along the line normal to the strut stent surface and extends with a sequence of n contiguous layers $[x_{i-1}, x_i]$ $i = 1, 2 \ldots, n$ from the polymer coating interface $x_0 = 0$ up to the wall bound x_n estimated by the penetration distance d^* (see Section 3). ST indicates the metallic stent strut bearing the coating (figure not in scale).

$c(x,t)$ (mg/ml) is considered. Since the metallic strut is impermeable to the drug, no mass flux passes through the boundary surface $x = x_{-1} = -l_0$. Moreover, it is assumed that the plasma does not penetrate the surface of the stent coating. Thus, the dynamics of the drug in the coating (1st layer) is described by the following 1D averaged diffusion equation, and related boundary-initial conditions:

$$\frac{\partial c_0}{\partial t} + \frac{\partial}{\partial x}\left(-D_0 \frac{\partial c_0}{\partial x}\right) = 0 \qquad \text{in } [x_{-1}, x_0] = [-l_0, 0]$$
$$-D_0 \frac{\partial c_0}{\partial x} = 0 \qquad \text{at } x = x_{-1}$$
$$c_0(x,0) = C_0 f_0(x) \tag{2.1}$$

where D_0 (cm^2/s) is the drug diffusivity and c_0 the concentration in the coating and $0 \leqslant f_0(x) \leqslant 1$.

In the i-th layer of the wall, the drug dynamics is described by the following advection–diffusion-reaction equation and related initial conditions:

$$\frac{\partial c_i}{\partial t} + \frac{\partial}{\partial x}\left(-D_i \frac{\partial c_i}{\partial x} + 2\delta_i c_i\right) + \beta_i c_i = 0 \quad \text{in } [x_{i-1}, x_i] \qquad i = 1, 2, \ldots, n$$
$$c_i = 0 \qquad \text{at } t = 0 \tag{2.2}$$

where D_i(cm^2/s) is the diffusivity of drug and c_i its concentration in the i-th layer and $2\delta_i$ (cm/s) accounts for a constant characteristic convection parameter. It may be estimated as $2\delta_i = \dfrac{\alpha_i u_i}{\epsilon_i}$ [4], where α_i is the hindrance coefficient in the x-direction [17], ϵ_i the porosity and u_i is the filtration velocity due to the pressure difference between lumen and adventitia. Note that $2\delta_i$ can be rewritten as $2\delta_i = (1 - v_i)u_i$, being $v_i = 1 - \dfrac{\alpha_i}{\epsilon_i}$ the Stavernan filtration coefficient [18].

The last term on the l.h.s. of the first of Eqs. (2.2) represents the drug reaction on the surface of smooth muscle cells (SMCs) inside the media layer. Here, it is approximated by a linear reaction having $\beta_i > 0$ (s^{-1}) as an effective first-order consumption rate coefficient. To close the previous mass transfer system of Eq. (2.2), flux and concentration continuity conditions have to be assigned at each layer interface $x = x_i$:

$$\frac{c_i}{k_i \epsilon_i} = \frac{c_{i+1}}{k_{i+1}\epsilon_{i+1}} \qquad D_i \frac{\partial c_i}{\partial x} - 2\delta_i c_i = D_{i+1}\frac{\partial c_{i+1}}{\partial x} - 2\delta_{i+1} c_{i+1}$$
$$\text{at } x = x_i \qquad i = 1, 2, \ldots, n-1 \tag{2.3}$$

where k_i is the partition coefficient.

In addition, to slow down the drug release rate, a permeable membrane (called *topcoat*) of permeability P (cm/s) is located at the interface ($x = 0$) between the coating and the arterial wall. A continuous mass flux passes through it orthogonally to the coating film with a possible concentration jump. In the present case, the mass transfer through the topcoat can be described using the second Kedem–Katchalsky equation [19], that is:

$$-D_0 \frac{\partial c_c}{\partial x} = P\left(\frac{c_0}{k_0 \epsilon_0} - \frac{c_1}{k_1 \epsilon_1}\right) \qquad \text{at } x = 0 \tag{2.4}$$
$$D_0 \frac{\partial c_0}{\partial x} = D_1 \frac{\partial c_1}{\partial x} - 2\delta_1 c_1 \qquad \text{at } x = 0 \tag{2.5}$$

As reported in [11], only in the media layer the convection-reaction terms are relevant, whereas in the other layers these effects can be neglected. However, it has been shown that a more general model including convection-reaction terms is amened to a pure diffusive system by a variable transformation [13]. Finally, a boundary condition has to be imposed at the limit of adventitia x_n. Some controversy occurs when measuring this wall bound. Different values of the thickness are in fact given in literature, depending on the arterial size and generally a range $100 - 200$ μm is found for a medium sized artery [6,11,17,20]. Actually, as the arterial wall is embedded in the surrounding tissues, the drug transport does not stop at the adventitia but proceeds forward in the external tissues, at a distance that depends on time when the process is observed. In principle, the domain where diffusion takes place cannot be estimated a priori and any truncation of the domain is rather arbitrary, if made on physiological consideration only. As a matter of fact, for pure diffusion processes where concentration and mass flux vanish asymptotically, instead of guessing the correct wall thickness, a rigorous and general modelling is made by considering a semi-infinite medium ($x_n \to \infty$) in perfect contact with the arterial media and having uniform properties (equal to those of the last layer, i.e. the adventitia).

Thereby the concentration and mass flux for $x \to \infty$ equate their initial value there, say zero, and the boundary conditions can be posed as:

$$\lim_{x\to\infty} c_n = 0 \qquad \text{or} \qquad \lim_{x\to\infty} \frac{\partial c_n}{\partial x} = 0 \tag{2.6}$$

3. Penetration distance and time

For computational purposes, we do not model the outmost layer as a semi-infinite medium, but we consider a convenient limited portion of it and by approximating the Eq. (2.6) using the similar concept of penetration distance for transient, heat diffusive problems [15]. Because of the strong analogy between heat and mass transfer problems, the above definition is revisited here for mass-diffusion processes and extended to multi-layers transient problems. The idea is based on observing that the concentration is damped out asymptotically (within a given tolerance) over a short

distance at the small times, whereas this distance increases at larger times. More precisely, let us consider a *large* (say semi-infinite) porous homogeneous medium $x \geqslant 0$, having diffusion coefficient D_1, and with an initial zero concentration. Faced in perfect contact with it, an infinite reservoir is located at $x \leqslant 0$, and contains a substance at concentration c_0. It is known that the mass diffuses through the medium and its concentration $c(x,t)$ tends asymptotically to zero for $x \to \infty$. Given a tolerance $\varepsilon = 10^{-m}$, the *penetration depth* d^* at a given time t is defined as the distance where the concentration and the mass flux $J = -D_1 \dfrac{\partial c}{\partial x}$ vanish within the prescribed tolerance, that is $c(x,\cdot)$ and $J(x,\cdot)$ stay below a sufficiently *small* value such as $10^{-m}c_0$ and $10^{-m}J_0$, respectively. Analogously, the *penetration time* t^* at a given location x is the time that it takes so that $c(\cdot,t)$ (resp. $J(\cdot,t)$) remain below $10^{-m}c_0$ (resp. $10^{-m}J_0$) in the filling process.

Similarly to the thermal problems, it can be proved by numerical experiments that in a single layer mass-diffusion process, the penetration distance $d^*(t)$ is estimated by [15]:

$$d^* \simeq \sqrt{10mD_1 t} \quad t > 0 \tag{3.1}$$

It measures the minimum distance from $x = 0$ such that $c(d^*,t)/c_0 \simeq J(d^*,t)/J_0 \lesssim 10^{-m}$. Reciprocally, the penetration time $t^*(x)$ is computed as:

$$\frac{D_1 t^*}{x^2} \simeq \frac{0.1}{m} \quad x \geqslant 0 \tag{3.2}$$

The idea can be generalized to $n-1$ adjoining layers $[x_{i-1}, x_i]$, $i = 1, \ldots, n-1$, faced with a n-th semi-infinite layer $[x_{n-1}, \infty[$, having diffusion coefficients D_i and in perfect contact with an infinite reservoir at $x = 0$. The penetration time $t^*(x)$ and the distance $d^*(t)$ are given, respectively, by:

$$\frac{t^*}{\left[\sum_{j=1}^{i-1} \dfrac{l_j(1-\delta_{ij})}{\sqrt{D_j}} + \dfrac{x - x_{i-1}}{\sqrt{D_i}}\right]^2} \simeq \frac{0.1}{m} \qquad \text{for } x \geqslant x_{i-1} \qquad i = 1 \ldots, n \tag{3.3}$$

$$d^* \simeq \sqrt{10mD_i t} + \sum_{j=1}^{i-1} l_j(1-\delta_{ij})\left(1 - \prod_{s=j}^{i-1}\sqrt{\frac{D_{s+1}}{D_s}}\right)$$
$$\text{for } t \geqslant t^*(x_{i-1}) = t^*_{i-1} \qquad i = 1 \ldots, n \tag{3.4}$$

with δ_{ij} the Kronecker symbol (see Appendix A.1 for a proof in the case $n = 2$). In a n-layered wall, for $t \leqslant t^*_i$ only the first i-th layers will be considered and the condition $c_i = 0$ is imposed at $x = x_i$. For $t > t^*_{n-1}$, the n-th semi-infinite layer can be truncated at the penetration distance $x_n = d^*(t_{n-1})$ and the asymptotic conditions (2.6) are replaced by

$$c_n = 0 \qquad \text{or} \qquad \frac{\partial c_n}{\partial x} = 0 \qquad \text{at } x_n = d^* \tag{3.5}$$

within an accuracy of 10^{-m}, with d^* defined in Eq. (3.4) for a boundary accuracy index (BAI) m. In other words, setting condition (3.5) guarantees that the concentration and the mass flux vanish at d^* with a mass loss comparable with 10^{-m}. In the outmost n-th layer, both the above conditions hold, but the absorbing condition $c_n = 0$ is expected to be more realistic, since the vasa vasorum of the adventitia are continually replenished with fresh blood and sweep away any residual drug [6].

4. Solving procedure

The classical separation of variables (SOV) method is used to solve the model equations. Before that, it is convenient to rewrite the equations in a dimensionless form.

4.1. Scaling

All the variables, the parameters and the equations are now normalized to get easily computable nondimensional quantities as follows:

$$\bar{x} = \frac{x}{d^*} \qquad \bar{l} = \frac{l}{d^*} \qquad \bar{t} = \frac{D_{max}}{(d^*)^2}t \qquad \bar{c}_i = \frac{c_i}{C_0}$$
$$\gamma_i = \frac{D_i}{D_{max}} \qquad \phi = \frac{Pd^*}{D_{max}(k\epsilon)_{max}} \qquad \sigma_i = \frac{(k\epsilon)_i}{(k\epsilon)_{max}} \tag{4.1}$$

where subscript max denotes the maximum value across the $n+1$ layers. By means of the following change of variables:

$$\bar{x} \to x \qquad \bar{l} \to l \qquad \bar{t} \to t \qquad \bar{c}_i \to c_i$$

the problem (2.1)–(2.2) can be written in dimensionless form as:

$$\frac{\partial c_i}{\partial t} = \gamma_i \frac{\partial^2 c_i}{\partial x^2} \qquad \text{in } [x_{i-1}, x_i] \qquad i = 0, 1, \ldots, n \tag{4.2}$$

with the initial conditions:

$$c_0(x,0) = f_0(x) \qquad c_i(x,0) \qquad i = 1, \ldots, n \tag{4.3}$$

and with the following interface and B.C.'s:

$$\frac{\partial c_0}{\partial x} = 0 \qquad \text{at } x = x_{-1} = -l_0$$
$$\gamma_0 \frac{\partial c_0}{\partial x} = \gamma_1 \frac{\partial c_1}{\partial x} \qquad -\gamma_0 \frac{\partial c_0}{\partial x} = \phi\left(\frac{c_0}{\sigma_0} - \frac{c_1}{\sigma_1}\right) \qquad \text{at } x = 0$$
$$\frac{c_i}{\sigma_i} = \frac{c_{i+1}}{\sigma_{i+1}} \qquad \gamma_i \frac{\partial c_i}{\partial x} = \gamma_{i+1}\frac{\partial c_{i+1}}{\partial x} \qquad \text{at } x = x_i \qquad i = 1, 2 \ldots, n-1$$
$$c_n = 0 \quad \text{at } x = 1 \tag{4.4}$$

The nondimensional penetration time and depth for a n-layer system are defined similarly as done in Eqs. (3.3) and (3.4).

4.2. The eigenvalue problem

Because of discontinuous coefficients of the piecewise-homogeneous layers, the SOV method leads to a Sturm–Liouville problem which is not of traditional type, as shown below. By separation of variables we have:

$$c_i = X_i(x)G_i(t) \qquad i = 0, 1 \ldots, n \tag{4.5}$$

and

$$\frac{X_i''(x)}{X_i(x)} = \frac{G_i'(t)}{\gamma_i G_i(t)} = -\lambda_i^2 \tag{4.6}$$

where the constants λ_i are the separation constants, each referring to its own layer. Solution of the previous equations leads to:

$$G_i(t) = \exp(-\lambda_i^2 \gamma_i t) \tag{4.7}$$

and

$$X_i(x) = a_i \cos(\lambda_i x) + b_i \sin(\lambda_i x) \tag{4.8}$$

By imposing $G_0 = G_1 = \cdots = G_n$, one gets:

$$\lambda_i = \sqrt{\frac{\gamma_0}{\gamma_i}}\lambda_0 \qquad i = 1, \ldots, n \tag{4.9}$$

and by the B.C.'s:

$$a_0\sin(\lambda_0 l_0)+b_0\cos(\lambda_0 l_0)=0 \tag{4.10}$$

$$\gamma_0 b_0\lambda_0=\gamma_1 b_1\lambda_1 \tag{4.11}$$

$$-\gamma_0 b_0\lambda_0=\phi\left(\frac{a_0}{\sigma_0}-\frac{a_1}{\sigma_1}\right) \tag{4.12}$$

$$\frac{1}{\sigma_i}(a_i\cos(\lambda_i x_i)+b_i\sin(\lambda_i x_i))=\frac{1}{\sigma_{i+1}}(a_{i+1}\cos(\lambda_{i+1}x_i)+b_{i+1}\sin(\lambda_{i+1}x_i)) \tag{4.13}$$

$$\sqrt{\gamma_i}[b_i\cos(\lambda_i x_i)-a_i\sin(\lambda_i x_i)]=\sqrt{\gamma_{i+1}}[b_{i+1}\cos(\lambda_{i+1}x_i)-a_{i+1}\sin(\lambda_{i+1}x_i)]$$

$$i=1,2\ldots,n-1 \tag{4.14}$$

$$\cos(\lambda_n)a_n+\sin(\lambda_n)b_n=0 \tag{4.15}$$

This set of $2n+2$ algebraic equations form a homogeneous system with unknowns $a_i, b_i \quad i=0,1\ldots,n$. By imposing that the coefficient matrix be singular and by using Eq. (4.9), we get a relationship in λ_0 (eigencondition). The discontinuity of the coefficients due to the non smoothness of the layer diffusivities leads to irregularities within the entire spectrum of roots of the eigenvalue equation. Explicit approximate (but very accurate) equations are available for computing eigenvalues of Sturm–Liouville problems with discontinuous coefficients [21]. However, such solutions were derived for general mathematical studies and for a variety of non-mass-diffusion applications, such as applied mechanics, geophysics and oceanography, and these methods are inadequate for transient mass-diffusion problems in layered porous media. Here the eigencondition problem is solved numerically by a successive bisection method. It admits an infinite number of roots $(\lambda_0^k), k=1,2,\ldots$ and, from them, the whole set of eigenvalues $(\lambda_i^k), \quad i=1\ldots,n$, $k=1,2,\ldots$ is determined.

Subsequently, from each eigenvalue, the constants $a_i^k, b_i^k \quad i=n,n-1\ldots,1,0$ are obtained in cascade from Eq. (4.15)…,(4.10) as a function of an arbitrary value b_0^k (such a multiplicative constant b_0^k is determined through the initial condition Eq. (4.3)). Thus the eigenfunctions defined in Eq. (4.8) have the form:

$$X_i^k(x)=b_0^k\left[\tilde{a}_i^k\cos(\lambda_i^k x)+\tilde{b}_i^k\sin(\lambda_i^k x)\right]=b_0^k\widetilde{X}_i^k(x) \tag{4.16}$$

where $\tilde{a}_i^k=\dfrac{a_i^k}{b_0^k}$ and $\tilde{b}_i^k=\dfrac{b_i^k}{b_0^k}$.

5. Computing drug concentration and mass

Once the eigenvalues λ_0^k are computed, the corresponding time-variable functions G_i defined by Eq. (4.7) are obtained as:

$$G_i^k(t)=G_0^k(t)=\exp(-\gamma_0(\lambda_0^k)^2 t) \qquad i=1\ldots,n \tag{5.1}$$

Thus, the general solution of the problem (4.2)–(4.4) is given by a linear superposition of the fundamental solutions (4.16)–(5.1) in the form:

$$c_i(x,t)=\sum_{k=1}^{\infty}A_k\widetilde{X}_i^k(x)\exp(-\gamma_i(\lambda_i^k)^2 t)=\sum_{k=1}^{\infty}A_k\widetilde{X}_i^k(x)\exp(-\gamma_0(\lambda_0^k)^2 t) \tag{5.2}$$

where the Fourier coefficients $A_k:=b_0^k$ are computed in accordance with the initial condition. By evaluating Eq. (5.2) at $t=0$ and multiplying it by $\widetilde{X}_i^h$, after integration we get:

$$\int_{x_{i-1}}^{x_i}\sum_k A_k\widetilde{X}_i^k\widetilde{X}_i^h\,dx=\int_{x_{i-1}}^{x_i}f_i(x)\widetilde{X}_i^h\,dx \qquad h=1,2,\ldots. \tag{5.3}$$

By combining Eq. (5.3) over the $n+1$ layers through the coefficients $\dfrac{1}{\sigma_i}$, and by using the orthogonality property (see Appendix A.2), we have:

$$A_k\left(\sum_{i=0}^{n}\frac{1}{\sigma_i}\int_{x_{i-1}}^{x_i}(\widetilde{X}_i^k)^2\,dx\right)=\sum_{i=0}^{n}\frac{1}{\sigma_i}\int_{x_{i-1}}^{x_i}f_i(x)\widetilde{X}_i^k\,dx \tag{5.4}$$

where the term in brackets on the l.h.s. is the norm $\widetilde{N}_k$ (see Appendix A.2). Because of the initial condition Eq. (4.3) (i.e., the drug is initially contained only in the coating layer), the summation on the r.h.s. of Eq. (5.4) reduces to the first term only. In particular, when the drug is uniformly distributed in the coating, i.e. $f_0(x)=1$, bearing in mind Eq. (4.10) and integrating from $-l_0$ to 0, we have:

$$A_k=\frac{\tilde{a}_0^k\sin(\lambda_0^k l_0)+\tilde{b}_0^k(\cos(\lambda_0^k l_0)-1)}{\sigma_0\widetilde{N}_k\lambda_0^k}=-\frac{1}{\sigma_0\widetilde{N}_k\lambda_0^k}$$

$$k=1,2,\ldots. \tag{5.5}$$

The analytical form of the last equations allows an easy computation of the dimensionless drug mass (per unit of area) in both coating and wall layers as function of time as:

$$M_0(t)=\int_{-l_0}^{0}c_0(x,t)dx \quad M_i(t)=\int_{x_{i-1}}^{x_i}c_i(x,t)dx \quad M_w(t)=\sum_{i=1}^{n}M_i(t)$$

We have:

$$M_0(t)=\sum_k-\frac{A_k}{\lambda_0^k}\exp(-\gamma_0(\lambda_0^k)^2 t) \tag{5.6}$$

$$M_i(t)=\sum_k A_k\frac{\exp(-\gamma_i(\lambda_i^k)^2 t)}{(\lambda_i^k)^2}\left[\frac{d\widetilde{X}_i^k}{dx}(x_{i-1})-\frac{d\widetilde{X}_i^k}{dx}(x_i)\right]=\sum_k A_k\frac{\tilde{a}_i^k[\sin(\lambda_i^k x_i)-\sin(\lambda_i^k x_{i-1})]-\tilde{b}_i^k[\cos(\lambda_i^k x_i)-\cos(\lambda_i^k x_{i-1})]}{\lambda_i^k}\times\exp(-\gamma_i(\lambda_i^k)^2 t) \tag{5.7}$$

In particular, we have:

$$M_0(0)=l_0 \qquad M_i(0)=0 \qquad i=1,2\ldots,n \tag{5.8}$$

Moreover, Eq. (5.7) shows that $\lim_{t\to\infty}M_i(t)=0$ for all layers, except for the last one. The n–th layer thickness tends to ∞ as $t\to\infty$ and the expression in Eq. (5.7) does not hold for it. In such a case, $M_n\propto\operatorname{erfc}\left(\frac{const.}{\sqrt{t}}\right)$ and this implies that $\lim_{t\to\infty}M_n(t)=M_0(0)$ (see Appendix A.1). Summing over all the layers 1,2…,n the terms correspondent to intermediate layers cancel out and we have:

$$M_w(t)=\sum_k A_k\exp(-\gamma_i(\lambda_i^k)^2 t)\left[\frac{1}{(\lambda_1^k)^2}\frac{d\widetilde{X}_1^k}{dx}(0)-\frac{1}{(\lambda_n^k)^2}\frac{d\widetilde{X}_n^k}{dx}(1)\right]=\sum_k A_k\exp(-\gamma_i(\lambda_i^k)^2 t)\left[\frac{\tilde{b}_1^k}{\lambda_1^k}-\frac{\tilde{b}_n^k\cos(\lambda_n)-\tilde{a}_n^k\cos(\lambda_n)}{\lambda_n^k}\right] \tag{5.9}$$

Table 1
The parameters used in the simulations for the coating and the wall layers. The penetration distance d^* estimates the wall bound, provides the thickness l_5 of the external layer and depends on the maximum simulated time and on BAI index m (see Eq. (3.4) and Table 3).

	Coating (0)	Endothelium (1)	Intima (2)	IEL (3)	Media (4)	Adventitia (5)
$l_i=x_i-x_{i-1}$ (cm)	5×10^{-4}	2×10^{-4}	10^{-3}	2×10^{-4}	2×10^{-2}	d^*-x_4
D_i (cm^2/s)	10^{-10}	8×10^{-9}	7.7×10^{-8}	4.2×10^{-8}	7.7×10^{-8}	12×10^{-8}
ϵ_i	0.1	5×10^{-4}	0.61	4×10^{-3}	0.61	0.85
k_i	1	1	1	1	1	1

Table 2
Penetration times t_i^* $i = 1, 2, 3, 4$ (in s) for different BAI.

m	t_1^*	t_2^*	t_3^*	t_4^*
2	0.25	1.705	2.322	311.187
5	0.1	0.682	0.929	124.47
8	0.0625	0.4262	0.5806	77.796

Table 3
Penetration distances d^* (cm) at several times (s) for m = 2,5,8. In all cases d^* falls within the 5-th layer ($d^* \geqslant x_4 = 0.0214$ cm) (cfr. tab. 2).

m \t	500	1000	3000	10000	20000
2	0.0287	0.0430	0.0789	0.1489	0.2131
5	0.0488	0.0715	0.1282	0.2390	0.3404
8	0.0633	0.0920	0.1637	0.3039	0.4322

6. Numerical results

Following [11,14], let us consider the arterial wall subdivided in four layers: endothelium (1) intima (2), IEL (3), media (4), in contact with the adventitia and external tissues (5). Despite of the low geometrical dimension, a large number of parameters influences the problem and a complete characterization of the physiological setting remains a difficult task. Each parameter is interconnected with the others and influences the global solution. Actually, the previous analysis shows that the problem depends only on the independent groups γ_i, ϕ, σ_i and x_i defined by Eq. (4.1). In particular, the identification of all diffusive coefficients relative to a specific drug and within each layer is a demanding issue. To set up a realistic simulation, the parameters given in Table 1 and:

$$P = 10^{-6}\ \text{cm/s} \qquad f_0(x) = 1 \tag{6.1}$$

have been chosen in agreement with the typical scales in DES and data in literature for the arterial wall and heparin drug in the coating layers [2,11,17,20,22].

By using the data in Table 1, the penetration times at each layer interface (see Eq. (3.3)) are estimated in Table 2.

All the series appearing in the solution (see Eq. (5.2) and foll.) have been truncated at a finite number of terms M. A value of $M = 50$ is considered for all times reported in the simulation. The penetration distance which corresponds to the maximum simulated time (2×10^4 s) falls beyond $x_4 = 0.0214$ cm in all cases (Table 3). For all m, the outmost layer results much thicker than the other ones ($\simeq l_4 \times 10$ at time $t = 2 \times 10^4$ s, in the case

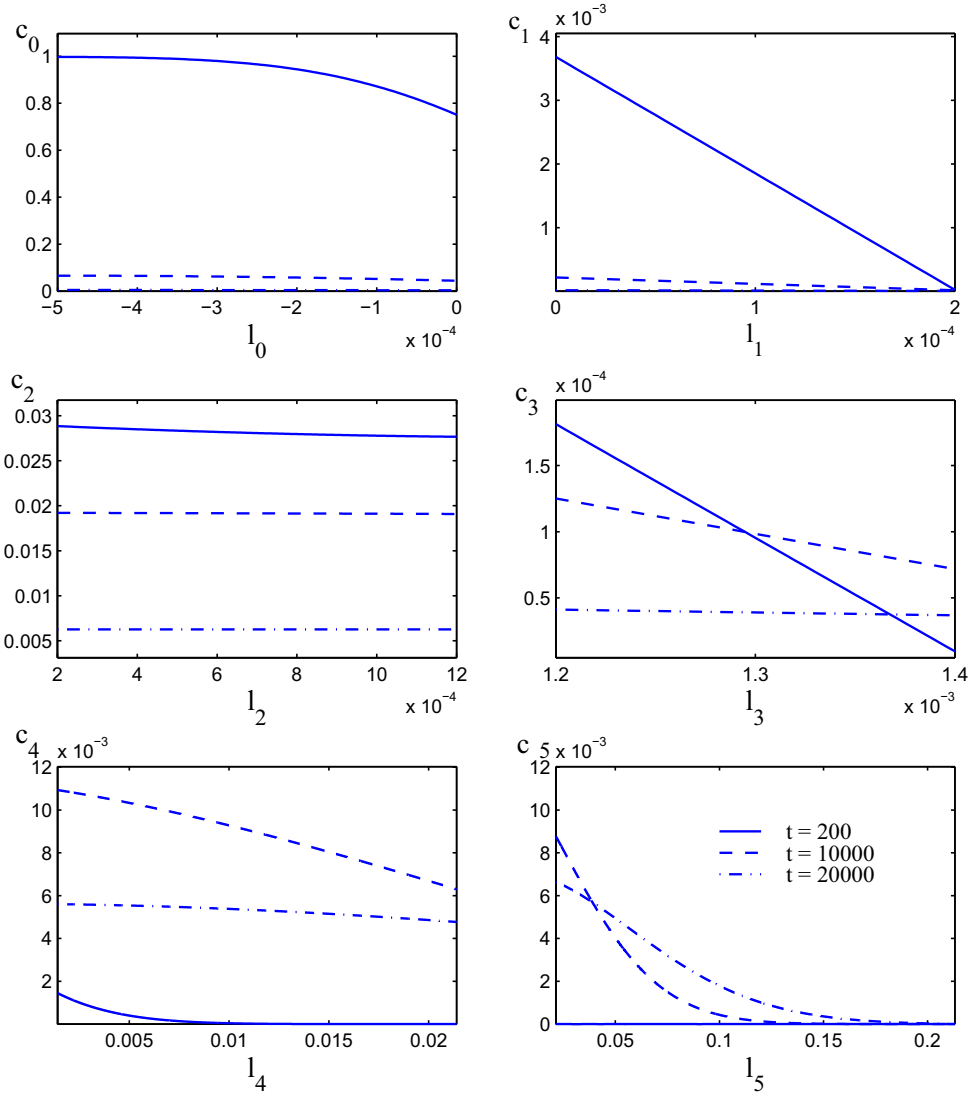

Fig. 3. Concentration profiles in the six layers at three instants (in s) (note the different scale for coordinates and concentrations).

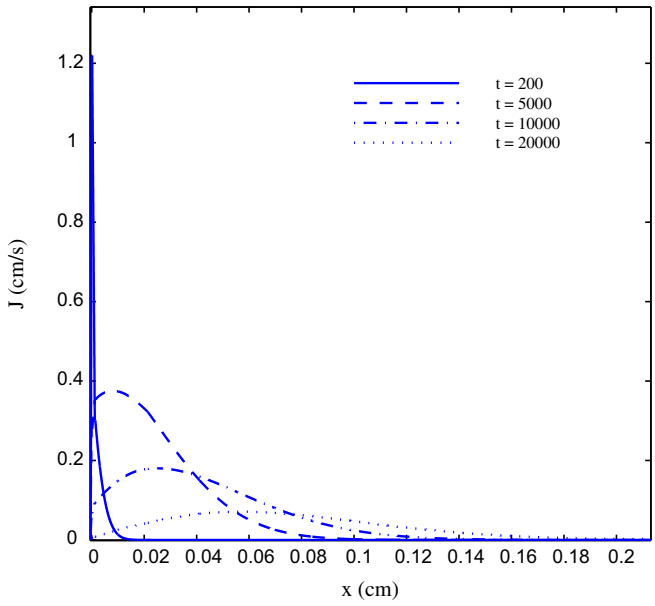

Fig. 4. Distribution of the mass flux through the wall section at four instants (in s). The peak of mass flux travels from the inner to the outer layers and drops with time. Note the sharp boundary layer at the innermost layers.

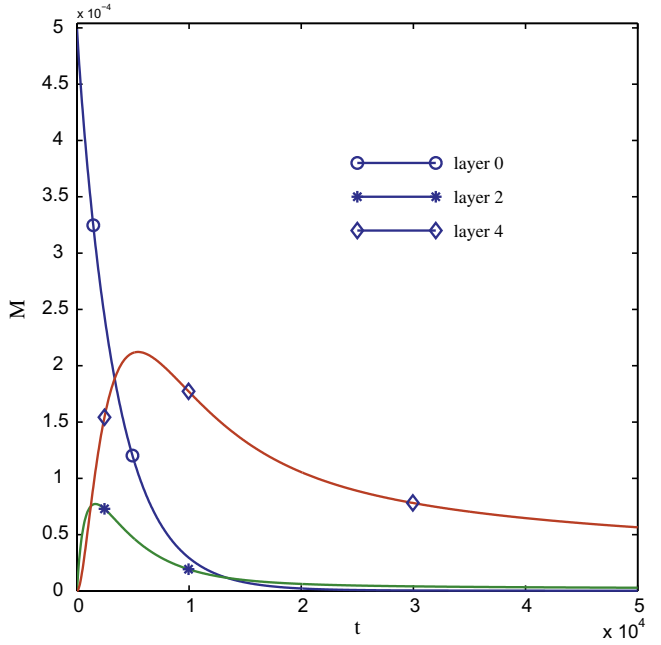

Fig. 5. Dimensionless mass in the coating (layer 0), endothelium (layer 2) and media (layer 4) vs. time (in s). In the coating mass is monotonically decreasing, while in the others there is a characteristic time at which the drug reaches a peak.

Table 4
Percentage of the drug mass retained in each layer at different times (in s ≃ (d : h : m)).

t	θ_0 (%)	θ_1 (%)	θ_2 (%)	θ_3 (%)	θ_4 (%)	θ_5 (%)
2000 (≃ 33m)	55	< 0.01	15	< 0.01	25	3.2
5000 (≃ 1h : 23m)	23	< 0.01	9.4	<0.01	42	24
10^4 (≃ 2h : 47m)	5.8	< 0.01	3.8	<0.01	35	54
2×10^4 (≃ 5h : 33m)	0.4	< 0.01	1.2	<0.01	21	77
5×10^4 (≃ 13h : 53m)	< 0.01	< 0.01	0.5	<0.01	11	87
10^5 (≃ 1d : 4h)	< 0.01	< 0.01	0.3	<0.01	7.6	91
5×10^5 (≃ 5d : 19h)	< 0.01	< 0.01	0.1	<0.01	3.3	96
10^6 (≃ 11d : 14h)	< 0.01	< 0.01	0.1	<0.01	2.3	97
5×10^6 (≃ 57d : 21h)	< 0.01	< 0.01	0.05	<0.01	1.0	98

$m = 2$) and needs a high number of grid points to be conveniently resolved. However, numerical results show negligible differences with m, present only in the outmost layer at higher times. For our purposes, a BAI $m = 2$ is sufficient to compute a penetration distance that guarantees a good solution accuracy without computational overhead.

Drug is retained differently in each layer, which receives mass from the inner and transmits to the outer, in a cascade sequence, up to be completely damped out at distance d^* that constitutes the wall bound. Concentration is decreasing inside each layer, being possibly discontinuous at the interfaces, with the mass flux continuity preserved (Figs. 3, 4). Interestingly enough, the levels of concentration in layer 2 (intima) are nearly constant and can be higher than in the others, at intermediate times. This is in agreement with the higher diffusivity D_2 and relatively small layer thickness l_2.

We compute the fraction of drug mass retained in each layer, defined as:

$$\theta_i(t) = \frac{M_i(t)}{M_0(0)} \qquad i = 0, 1, \ldots, 5 \tag{6.2}$$

and Table 4 shows its different distribution in the wall layers. Having posed the first boundary condition (3.5), a negligible mass loss occurs out of the wall bound d^*. In other words, due to the absorbing condition (3.5), all drug mass is transferred at the outmost layer at a sufficiently large time and the total mass is preserved and equals its initial value (say the drug mass in the coating $M_0(0)$):

$$\frac{M_0(0) - \sum_{i=0}^{5} M_i(t)}{M_0(0)} = 1 - \sum_{i=0}^{5} \theta_i(t) \propto 10^{-m} \tag{6.3}$$

Thus, any truncation of the domain before d^* is arbitrary and does not ensure a conservative model.

Due to the diffusive coefficient and to the porosity, the mass is exponentially decreasing in the coating and in the (1) (innermost layers), but is first increasing up to some upper bound and then decaying asymptotically in the (2), (3), and (4) (outer layers) (Fig. 5). In the outmost layer (5) the mass accumulates as the time proceeds. The simulation points out the time of peak mass in the intima (layer 2) is at 1640 s (≈ 27 min), in the media (layer 4) is 5460 s (≈ 1 h: 30 min). The thin layers 1 and 3 retain a negligible mass due to their thickness, and the media is completely emptied ($\theta_4 \approx 1\%$) after a time of about 57 days (last row in Table 4). At that time, all the mass is transferred to the external wall layer, with a slight mass loss (Fig. 5). However, the therapeutic effects of DES is limited in the endothelium-media, while the residual drug in the outmost layer is considered lost.

Differently than in other single layer models, the current simulation constitutes a simple tool to predict the accurate concentration levels in each wall layer. These results can be used to assess whether drug reaches target tissues, and to optimize the dose capacity given by thin surface coatings for an extended period of time.

7. Conclusions

Mathematical modelling has emerged in recent years as a powerful tool to simulate drug delivery processes in DES and much effort is currently addressed for a deeper understanding of the elution mechanism. Such a phenomenon is not completely understood and may be influenced by different concurrent physical processes. One of them is the structure of the arterial wall that is

recognized constituted by a sequence of adjacent layers. The multi-layered wall accounts for a relatively detailed structure for the macromolecular transport inside the biological tissues and provides a better accuracy when compared with a homogeneous monolayered model in diffusion process for DES.

Even though a complete study needs a coupling with the blood flow and the mechanics of the stent, a simplified release model provides a deep insight into the complex physics of diffusion process into the wall layers. As a matter of fact, the analysis of a 1D model retains the basic ingredients of the underlying physics and has revealed to provide much understanding on the mechanism of mass diffusion.

By showing the relationship among the several variables and material parameters, it can be used to identify simple indexes or clinical indicators of biomedical significance and to optimize drug elution for a desired targeted tissue. A characteristic simulation parameter is the penetration depth, defined as the distance beyond which the concentration and mass flux reduce to a given percentage of the boundary value at a given time. The model turns out to be very sensitive to the manifold physico-chemical and physiological parameters and their correct identification is a critical issue and constitutes the key for its successful use. An additional effort is required to determine them for each arterial wall layer more accurately. As long as built on a realistic set up, the current simulation is able to estimate the local concentration, offers an easy tool for computing the residence time of a drug and can be used as a guideline for designing better delivery systems in the arterial tissue. Although applied to the drug transport of DES, the present model can be easily extended to any other multi-layered mass transfer process.

Acknowledgments

The work has been partially supported by the CNR project *Bioinformatics*, 2009.

Appendix A

A.1. Penetration depth and time for two faced layers

Let us consider two faced layers $[0,x_1],[x_1,\infty[$, having diffusion coefficient D_1 (resp. D_2), with initial concentration $c_1(x,0)=c_2(x,0)=0$ and in perfect contact with an infinite reservoir c_0 extending for $x\leqslant 0$ (as consequence, the boundary condition $c_1(0,t)=c_0$ holds). Let us prove that the penetration time and depth, as defined in Eqs. (3.3)–(3.4) (with $n=2$ and $i=2$), can be estimated as:

$$\frac{t^*}{\left[\frac{l_1}{\sqrt{D_1}}+\frac{x-x_1}{\sqrt{D_2}}\right]^2}\simeq\frac{0.1}{m}\qquad \text{for } x\geqslant x_1 \tag{A.1}$$

and

$$d^*\simeq\sqrt{10mD_2t}+l_1\left(1-\sqrt{\frac{D_2}{D_1}}\right)\qquad \text{for } t\geqslant t^*(x_1)=t_1^* \tag{A.2}$$

(note that in this case, $x_1=l_1$).

For an analogous heat diffusive problem, an analytical solution is available in [23], pag. 409. Therefore, we can write:

$$\frac{c_2(x,t)}{c_0}=\frac{2}{K_1+1}\sum_{n=1}^{\infty}\left(\frac{K_1-1}{K_1+1}\right)^{n-1}\operatorname{erfc}\left[\frac{(2n-1)l_1}{2\sqrt{D_1t}}+\frac{x-l_1}{2\sqrt{D_2t}}\right]\quad \text{for } x\geqslant x_1 \tag{A.3}$$

where

$$K_1=\sqrt{\frac{D_2}{D_1}}$$

Note that for a perfect insulator ($D_2=0$) we obtain that $K_1=0$, which is the same as for a 1D finite plate insulated at $x=x_1=l_1$. When the material is an ideal diffuser ($D_2\to\infty$), we have that $K_1\to\infty$, which is the same as for a 1D finite plate kept at zero temperature at $x=l_1$.

For small dimensionless times, the dominant term of the above series is the first one and Eq. (A.3) simplifies to:

$$\frac{c_2}{c_0}\simeq\frac{2}{K_1+1}\operatorname{erfc}\left[\frac{l_1}{2\sqrt{D_1t}}+\frac{x-l_1}{2\sqrt{D_2t}}\right]\qquad \text{for } x\geqslant x_1 \tag{A.4}$$

According to the definition of penetration time, let the above concentration $\frac{c_2}{c_0}$ be a very small value such as 10^{-m}, $m=1,2,\ldots$, for a given $x>x_1$. Then, solving analytically Eq. (A.4) gives the penetration time as

$$\frac{t^*}{\left[\frac{l_1}{\sqrt{D_1}}+\frac{x-l_1}{\sqrt{D_2}}\right]^2}=\frac{1}{4\left[\operatorname{erfc}^{-1}\left(\frac{10^{-m}}{A}\right)\right]^2}\qquad x\geqslant x_1 \tag{A.5}$$

where $A=\frac{2}{1+K_1}$.

To approximate the r.h.s. of (A.5), let us note that $A\in[0,2]$ for $K_1\in[0,\infty]$. As a matter of fact, for $A=1$ and $m=10$, the r.h.s. of Eq. (A.5) gives the value of about 0.012. Some other values given by Eq. (A.5) are for $A=2$ and $m=10$, which yields 0.0116; and for $A=0.1$ and $m=10$ which yields 0.0134. Hence the values of the penetration time are quite insensitive to A, that is, to the diffusivity ratio. The most conservative value is $A=0.0116$ that, for sake of simplicity, is approximated by 0.01. In general, for any value of the integer m, we have:

$$\frac{1}{4\left[\operatorname{erfc}^{-1}\left(\frac{10^{-m}}{A}\right)\right]^2}\simeq\frac{0.1}{m} \tag{A.6}$$

which proves the r.h.s. of Eq. (A.1). By straightforward algebraic manipulation, we get Eq. (A.2). A similar result is obtained for $J_2(x,t)/J_0\simeq 10^{-m}$.

A.2. Orthogonality of the eigenfunctions

It is easily proved that the system of eigenfunction X_i^k is orthogonal [4], i.e.:

$$\sum_{i=0}^{n}\frac{1}{\sigma_i}\int_{x_{i-1}}^{x_i}\widetilde{X}_i^k\widetilde{X}_i^h dx=\begin{cases}0 & \text{for } k\neq h\\ \widetilde{N}_k & \text{for } k=h\end{cases} \tag{A.7}$$

where

$$\widetilde{N}_k=\sum_{i=0}^{n}\frac{1}{\sigma_i}\int_{x_{i-1}}^{x_i}(\widetilde{X}_i^k)^2dx \tag{A.8}$$

and

$$\int_{x_{i-1}}^{x_i}(\widetilde{X}_i^k)^2dx=\frac{1}{2}\left[x(\widetilde{X}_i^k)^2+\frac{1}{(\lambda_i^k)^2}\frac{d\widetilde{X}_i^k}{dx}\left(x\frac{d\widetilde{X}_i^k}{dx}-\widetilde{X}_i^k\right)\right]_{x_{i-1}}^{x_i} \tag{A.9}$$

Let us now prove the Eq. (A.9). By integration by parts, we have:

$$\int_{x_{i-1}}^{x_i}(\widetilde{X}_i^k)^2dx=\left[\widetilde{X}_i^k\int_{x_{i-1}}^{x_i}\widetilde{X}_i^k\right]_{x_{i-1}}^{x_i}-\int_{x_{i-1}}^{x_i}\left(\int\widetilde{X}_i^kdx\right)\frac{d\widetilde{X}_i^k}{dx}dx \tag{A.10}$$

Eq. (4.6) can be rewritten as:

$$X_i^k=-\frac{1}{(\lambda_i^k)^2}\frac{d^2\widetilde{X}_i^k}{dx^2} \tag{A.11}$$

and substituting in Eq. (A.10):

$$\int_{x_{i-1}}^{x_i}(\widetilde{X}_i^k)^2dx=\frac{1}{(\lambda_i^k)^2}\int_{x_{i-1}}^{x_i}\left(\frac{d\widetilde{X}_i^k}{dx}\right)^2dx-\frac{1}{(\lambda_i^k)^2}\left[\widetilde{X}_i^k\frac{d\widetilde{X}_i^k}{dx}\right]_{x_{i-1}}^{x_i} \tag{A.12}$$

On the other hand:

$$\int_{x_{i-1}}^{x_i}(\widetilde{X}_i^k)^2dx=\int_{x_{i-1}}^{x_i}1(\widetilde{X}_i^k)^2dx=[(\widetilde{X}_i^k)^2x]_{x_{i-1}}^{x_i}-2\int_{x_{i-1}}^{x_i}x\widetilde{X}_i^k\frac{d\widetilde{X}_i^k}{dx}dx \tag{A.13}$$

Making use of Eq. (A.11), the integral on the r.h.s. of the above Eq. yields

$$\int_{x_{i-1}}^{x_i}x\widetilde{X}_i^k\frac{d\widetilde{X}_i^k}{dx}dx=-\frac{1}{(\lambda_i^k)^2}\int_{x_{i-1}}^{x_i}x\frac{d\widetilde{X}_i^k}{dx}\frac{d^2\widetilde{X}_i^k}{dx^2}dx \tag{A.14}$$

Applying again the integration by parts:

$$\int_{x_{i-1}}^{x_i}x\frac{d\widetilde{X}_i^k}{dx}\frac{d^2\widetilde{X}_i^k}{dx^2}dx=\frac{1}{2}\left[x\left(\frac{d\widetilde{X}_i^k}{dx}\right)^2\right]_{x_{i-1}}^{x_i}-\frac{1}{2}\int_{x_{i-1}}^{x_i}\left(\frac{d\widetilde{X}_i^k}{dx}\right)^2dx \tag{A.15}$$

and substituting back Eq. (A.15) in Eqs. (A.14) and (A.13):

$$\int_{x_{i-1}}^{x_i}(\widetilde{X}_i^k)^2dx=\left[x(\widetilde{X}_i^k)^2\right]_{x_{i-1}}^{x_i}+\frac{1}{(\lambda_i^k)^2}\left[x\left(\frac{d\widetilde{X}_i^k}{dx}\right)^2\right]_{x_{i-1}}^{x_i}-\frac{1}{(\lambda_i^k)^2}\int_{x_{i-1}}^{x_i}\left(\frac{d\widetilde{X}_i^k}{dx}\right)^2dx \tag{A.16}$$

Finally, summing Eqs. (A.12) and (A.16), we obtain Eq. (A.9).

References

[1] W.H. Maisel, Unanswered questions: drug-eluting stents and the risk of late thrombosis, New Engl. J. Med. 356 (2007) 981–984.
[2] C. Creel, M. Lovich, E. Edelman, Arterial paclitaxel distribution and deposition, Circ. Res. 86 (8) (2000) 879–884.
[3] G. Athesian, M. Friedman, Integrative biomechanics: a paradigm for clinical applications of fundamental mechanics, J. Biomech. 42 (2009) 1444–1451.
[4] G. Pontrelli, F. de Monte, Mass diffusion through two-layer porous media: an application to the drug-eluting stent, Int. J. Heat Mass Transf. 50 (2007) 3658–3669.
[5] G. Vairo, M. Cioffi, R. Cottone, G. Dubini, F. Migliavacca, Drug release from coronary eluting stents: a multidomain approach, J. Biomech., in press, doi:10.1016/j.jbiomech.2010.01.033.
[6] R. Mongrain, L. Faik, et al., Effects of diffusion coefficients and struts apposition using numerical simulations for drug eluting coronary stents, J. Biomech. Eng. 129 (2007) 733–742.
[7] M. Grassi, G. Grassi, G. Pontrelli, L. Teresi, Novel design of drug delivery in stented arteries: a numerical comparative study, Math. Bio. Eng. 6 (3) (2009) 493–508.
[8] F. Migliavacca, F. Gervaso, M. Prosi, P. Zunino, S. Minisini, L. Formaggia, G. Dubini, Expansion and drug elution model of a coronary stent, Comp. Meth. Biomech. Biom. Eng. 10 (1) (2007) 63–73.
[9] M. Prosi, P. Zunino, K. Perktold, A. Quarteroni, Mathematical and numerical models for transfer of low-density lipoproteins through the arterial walls: a new methodology for the model set up with applications o the study of disturbed lumenal flow, J. Biomech. 38 (2005) 903–917.
[10] C. Vergara, P. Zunino, Multiscale boundary conditions for drug release from cardiovascular stents, Mult. Model Sim. 7 (2) (2008) 565–588.
[11] N. Yang, K. Vafai, Low-density lipoprotein (LDL) transport in an artery – a simplified analytical solution, Int. J. Heat Mass Transf. (2008) 497–505.
[12] M. Khakpour, K. Vafai, A critical assessment of arterial transport models, Int. J. Heat Mass Transf. 51 (2008) 807–822.
[13] G. Pontrelli, F. de Monte, Modelling of mass dynamics in arterial drug-eluting stents, J. Porous Media 12 (1) (2009) 19–28.
[14] M. Khakpour, K. Vafai, A comprehensive analytical solution of macromolecular transport within an artery, Int. J. Heat Mass Transf. (2008) 2905–2913.
[15] F. de Monte, J.V. Beck, D.E. Amos, Diffusion of thermal disturbances in two-dimensional Cartesian transient heat conduction, Int. J. Heat Mass Transfer 51 (2008) 5931–5941.
[16] A.C. Guyton, J.E. Hall, Textbook of Medical Physiology, 11th ed., Elsevier, 2007.
[17] P. Zunino, Multidimensional pharmacokinetic models applied to the design of drug-eluting stents, Cardiov. Eng. Int. J. 4 (2) (2004) 181–191.
[18] M. Khakpour, K. Vafai, Effects of gender-related geometrical characteristics of aorta-iliac bifurcation on hemodynamics and macromolecule concentration distribution, Int. J. Heat Mass Transf. 51 (2008) 5542–5551.
[19] A. Kargol, M. Kargol, S. Przestalski, The Kedem–Katchalsky equations as applied for describing substance transport across biological membranes, Cell. Mol. Biol. Lett. 2 (1996) 117–124.
[20] D.V. Sakharov, L.V. Kalachev, D.C. Rijken, Numerical simulation of local pharmacokinetics of a drug after intravascular delivery with an eluting stent, J. Drug Target 10 (6) (2002) 507–513.
[21] G.A. Athanassoulis, V.G. Papanicolau, Eigenvalue asymptotics of layered media and their applications to the inverse problem, SIAM J. Appl. Math. 57 (1997) 453–471.
[22] C. Hwang, D. Wu, E.R. Edelman, Physiological transport forces govern drug distribution for stent-based delivery, Circulation 104 (5) (2001) 600–605.
[23] A.V. Luikov, Analytical Heat Diffusion Theory, Academic Press, New York, 1968.